Dalton Transactions

PAPER

View Article Online
View Journal | View Issue

Cite this: *Dalton Trans.*, 2014, **43**, 13399

Versatile coordination chemistry of a bis(methyliminophosphoranyl)pyridine ligand on copper centres†

Thibault Cheisson and Audrey Auffrant*

Received 16th June 2014,
Accepted 15th July 2014

DOI: 10.1039/c4dt01794c

www.rsc.org/dalton

The coordination of a bis(methyliminophosphoranyl)pyridine ligand (**L**) to copper centres was studied. The use of copper(I) bromide precursors gave access to [**L**CuBr] (**2**) in which only one iminophosphorane arm is coordinated to the metal, as observed by X-ray crystallography and MAS ^{31}P NMR. Its fluxional behaviour in solution was demonstrated by VT-^{31}P NMR, and investigated by DFT calculations. On the other hand, coordination of **L** to $[Cu(CH_3CN)_4]PF_6$ gave a dimer $[\mathbf{L}_2Cu_2](PF_6)_2$ (**3**) in which the two copper centres do not have the same coordination sphere as shown by X-ray crystallography. Addition of a strong ligand such as PEt_3 allows the preparation of a cationic monomeric copper complex (**4**) in which **L** has a behaviour similar to that observed for **2**. Synthesis of copper(II) complexes was also achieved by chemical oxidation of **2**, which shows an irreversible oxidation at −0.36 *vs.* Fc^+/Fc, or directly *via* the coordination of **L** to $CuBr_2$. In [**L**$CuBr_2$] (**5**), **L** adopts a pincer coordination. Finally, the catalytic behaviour of copper(I) complexes **2** and **3** was investigated in cyclopropanation reactions and [3 + 2] cycloadditions.

Introduction

Over the past 3 decades, pincer ligands[1,2] have gained an important role in coordination chemistry with applications as sensors,[1,3] switches,[4] and catalysts.[5] This is related to their modularity allowing fine tuning of both their steric and electronic properties.[6] Various neutral pincer ligands incorporating three nitrogen donor functions with a central pyridine have been reported, among which are the well-known terpyridine[7] and bis(iminopyridine)[8] derivatives. Examples of such pincers incorporating iminophosphoranes have also been described (Fig. 1). Bochmann and coworkers used bis(iminophosphoranyl)pyridine (**A**, Fig. 1) complexes for ethylene polymerisation.[9] More recently, Wang studied the coordination chemistry of ligand **B** (Fig. 1) and the catalytic ability of some of its complexes for ε-caprolactone polymerisation.[10] Stephan and coworkers have explored the coordination of ligand **C** (Fig. 1) to palladium,[11] and have shown that the coordination by the nitrogen of the iminophosphorane functions allows a shielding of the metal by the exocyclic phosphorus substituents. We were therefore interested in studying the coordination

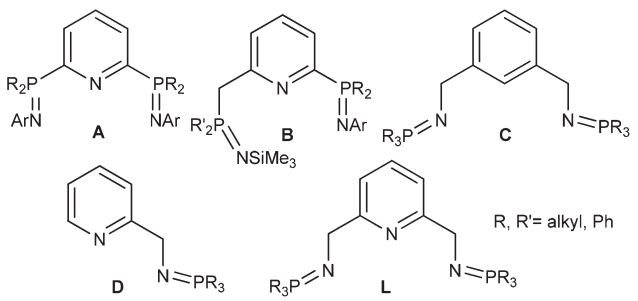

Fig. 1 Iminophosphorane-pyridine or -phenyl ligands.

behaviour of ligand **L**, which combines the protective ability of the peripheral triphenylphosphine groups, the electron donating capacity of iminophosphoranes, which act as strong σ and π donors with poor accepting properties, and a central pyridine. We thought that this core would balance the donation from iminophosphoranes thanks to its accepting capacity. **L** was described only recently[12] but its bidentate version (**D**, Fig. 1) has been employed for more than 10 years.[13,14] As Cadierno and coworkers recently highlighted the importance of the hemilability[15] of iminophosphorane ligands in their catalytic applications,[16] we were interested in studying such behaviour with **L** (Fig. 1), which should present a certain degree of flexibility thanks to the methylene linkers. Therefore we chose to investigate its coordination to copper centres. Indeed, coordination of iminophosphorane ligands to this metal was not much investigated and often restricted to anionic

Laboratoire de Chimie Moléculaire, Ecole Polytechnique, UMR CNRS 9168, F-91128 Palaiseau Cedex, France. E-mail: audrey.auffrant@polytechnique.edu

† Electronic supplementary information (ESI) available: VT-^{31}P NMR Eyring plot for **2** and **4**, X-ray structure of [**L**CuBr(MeCN)][$Ce(NO_3)_5$] (**6**), cyclic voltammogram of [**L**CuBr] (**2**), computational details. CCDC 996862–996866. For ESI and crystallographic data in CIF or other electronic format see DOI: 10.1039/c4dt01794c

ligands.[17] Actually, due to their electronic properties these ligands are more suitable to stabilise electron-deficient metals.[18]

The synthesis and characterisation of bis(methyliminophosphoranyl)pyridine copper(I) and copper(II) complexes are reported. The hemilability of **L** on Cu^{I} centres was studied using different techniques among which are solution and solid state NMR studies, X-ray analysis, and DFT calculations. Some of the synthesised complexes were also used as catalysts for two reactions: the alkene cyclopropanation and the [3 + 2] cycloaddition of an organic azide on alkynes.

Results and discussion

The pincer ligand **L** was easily prepared by a bromination/azidation sequence starting from 2,6-pyridinedimethanol yielding the bis-azide **1**, which was then reacted with triphenylphosphine (Scheme 1).[12] The ligand was isolated by precipitation in Et_2O in 78% overall yield, as no chromatographic purification is required, the synthesis is easily scalable to multigrams (up to 10 g). For the key step (formation of the N=P bond), we chose to rely on the Staudinger reaction rather than the Kirsanov reaction[11,19] because of the availability of the starting diol and the stability of **1**. Bis(methyliminophosphoranyl)pyridine **L** was characterised by multinuclear NMR and elemental analysis.

It exhibits a singlet at 9.9 ppm in $^{31}P\{^{1}H\}$ NMR in CD_2Cl_2 and a doublet ($^{3}J_{P,H}$ = 16.0 Hz) for the benzylic protons at 4.30 ppm in ^{1}H NMR in agreement with literature data.[12,13] As most iminophosphoranes, **L** is sensitive to moisture and decomposes in contact with air to the corresponding amine and triphenylphosphine oxide within minutes (in solution) and hours (in the solid state).

Synthesis of copper(I) complexes

Bis(methyliminophosphoranyl)pyridine ligand **L** was first reacted with various copper(I) bromide precursors (CuBr, [$CuBr(SEt_2)$] and [$CuBr(PPh_3)_3$]). In all cases, complex [**L**CuBr] (**2**) was formed as the sole product (Scheme 2), this requires few hours using [$CuBr(SEt_2)$] or [$CuBr(PPh_3)_3$] and overnight heating employing the poorly soluble polymeric CuBr. Interestingly, **L** was able to displace three triphenylphosphines. **2** is characterised in THF by a large singlet at 16.5 ppm in $^{31}P\{^{1}H\}$ NMR and a doublet at 4.24 ppm ($^{3}J_{P,H}$ = 11.5 Hz) in

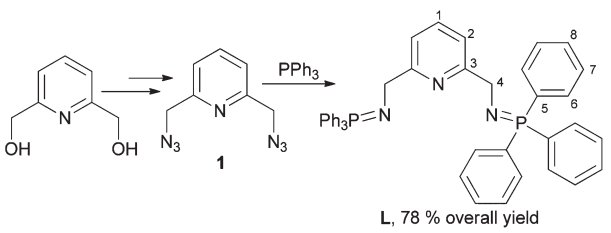

Scheme 1 Synthesis of the ligand **L**.

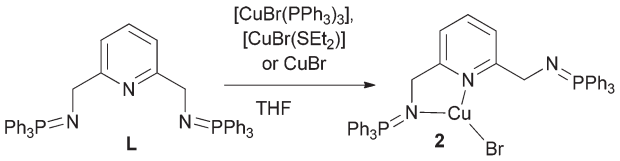

Scheme 2 Synthesis of complex **2**.

^{1}H NMR for the benzylic protons indicating a symmetric species in solution.

However X-ray analysis performed on single crystals of **2**, obtained by the slow diffusion of benzene into a concentrated THF solution, evidenced a non-symmetric structure (Fig. 2).

The copper center is only coordinated by the pyridine ring and one of the iminophosphorane groups, with the second one totally turned back without any interaction with the copper or other molecules in the packing. Therefore, the complex exhibits a trigonal geometry around the copper with a constrained metallocycle (N1–Cu1–N3: 82.7(1)°). The metal is almost coplanar with the pyridine ring (0.25 Å out of the plane), whereas the bromine and the coordinated nitrogen are slightly out of this plane with the N1–P1 bond almost coplanar to the Cu1–Br1 bond (8.7° of deviation). The two P–N bonds are not similar; indeed P1–N1 is longer than the non-coordinated P2–N2 (1.588(3) *vs.* 1.565(3) Å).

In order to establish whether this unsymmetrical structure is due to the crystallisation process or to insidious packing inside the crystal, we recorded a solid-state MAS ^{31}P NMR spectrum of a precipitated powder of **2** (Fig. 3, right), which shows two independent peaks at 8.0 ppm and 22.7 ppm. These are in agreement with the solid-state structure observed by X-ray diffraction; the non-coordinated iminophosphorane appears at 8.0 ppm (δ_P = 5.9 ppm in THF for **L**) and the coordinated one resonates at 22.7 ppm (*vide infra*). To gain further insight into the behaviour of **2** in solution, we performed variable temperature $^{31}P\{^{1}H\}$ NMR experiments in THF. The characteristic singlet of **2** starts to broaden around −70 °C and splits into two broad singlets at 24.4 and 9.5 ppm at −95 °C (Fig. 3, left).

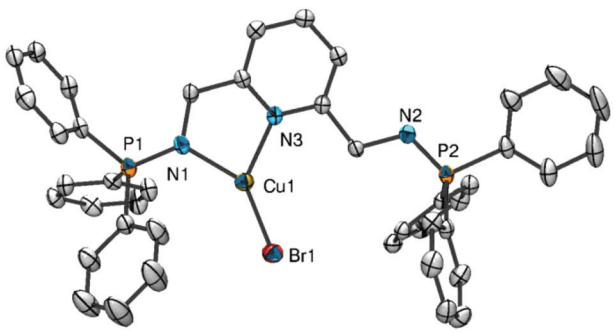

Fig. 2 ORTEP of the solid-state structure of **2** with 50% probability thermal ellipsoids. Hydrogens and one benzene solvent molecule were omitted for clarity. Selected bond lengths [Å] and angles (°): N1–Cu1 2.002(3), N3–Cu1 2.050(3), P1–N1 1.588(3), P2–N2 1.565(3), Cu1–Br1 2.2546(6); N1–Cu1–N3 82.7(1), N1–Cu1–Br1 141.17(8), N3–Cu1–Br1 135.37(8).

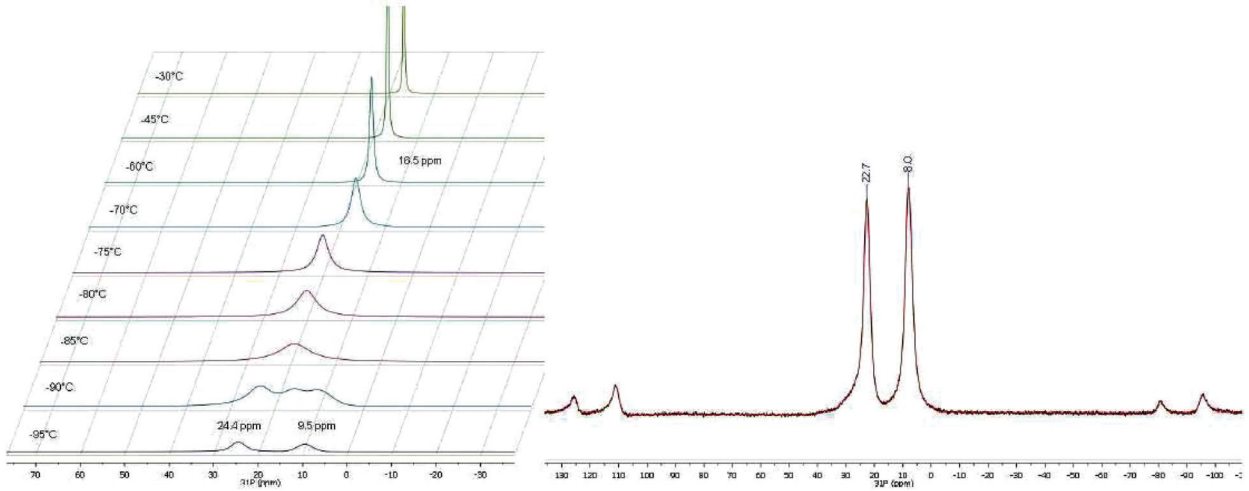

Fig. 3 VT $^{31}P\{^{1}H\}$ NMR of **2** in THF (left), MAS ^{31}P NMR spectrum of powdered **2** (right).

The exchange is too rapid to be completely blocked at this temperature; nevertheless, the coalescence was estimated around −90 ± 2 °C. An Eyring plot (see ESI†) allows the evaluation of the activation barrier of the process at 7.3(1) kcal mol^{-1}.

This exchange process was also investigated by DFT calculations, both associative and dissociative mechanisms were computed (see Fig. 4). Starting from **I** (the optimised structure of **2**), the dissociative pathway proceeds by the decoordination of the iminophosphorane leading to the linear intermediate **II**

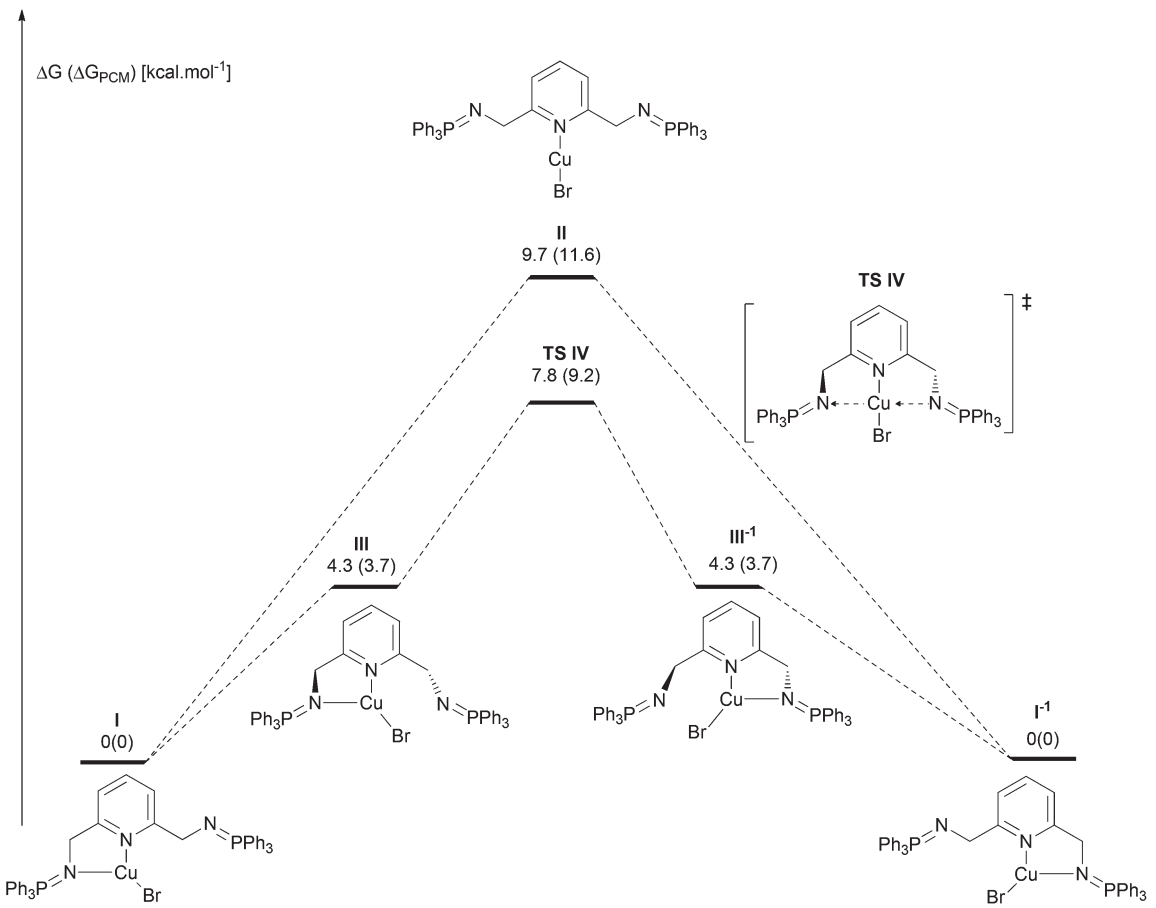

Fig. 4 Energetic profile of the computed exchange.

located at 9.7 kcal mol^{-1} above **I**. This value is slightly over the experimental one, especially if a solvation continuum is used (11.6 kcal mol^{-1}, standard PCM in THF). The second pathway proceeds through a concerted associative mechanism, a first minimum (**III**), in which the second iminophosphorane remains non-coordinated but has flipped on the copper side, was located by performing a relaxed scan on the nitrogen–copper distance. Despite the flatness of the energetic profile near this point, a transition state labelled **TS IV** (Fig. 4) was located at 7.8 kcal mol^{-1} above **I**. The latter value, in good agreement with the experimental one, validates the hypothesis of a concerted associative pathway.

This behaviour markedly differs from the hemilability of the pyridine moiety on copper(I) observed by van der Vlugt *et al.* using phosphine analogues of **L** (*i.e.* $R_2PCH_2(C_5H_3N)$-CH_2PR_2, R = Ph, ^{t}Bu). Moreover, upon halide abstraction they reported the isolation of a cationic T-shaped Cu^I complex.[20] When abstracting the bromine from **2**, a yellow solid poorly soluble in THF is obtained. Its $^{31}P\{^1H\}$ NMR spectrum evidences a sharp singlet at 28.8 ppm, which is in the range of the copper coordinated iminophosphorane, and a heptuplet at −144.1 ppm for the PF_6 counter-anion. The same complex **3** was synthesised by reacting **L** with a stoichiometric amount of $[Cu(CH_3CN)_4]PF_6$ in THF (Scheme 3).

The X-ray analysis of **3** (crystals were obtained by gas diffusion of pentane into an acetonitrile solution) did not show the expected T-shaped complex but the dimeric species as depicted in Fig. 5.

The coordination spheres of the two copper atoms are quite different; Cu1 is coordinated by two iminophosphorane groups in a nearly linear mode (N2–Cu1–N4: 173.7(1)°), whereas Cu2 exhibits a distorted tetrahedral geometry, with the coordination of the two pyridine rings and two iminophosphoranes. Such divergent geometries for two coppers were also observed by Piguet *et al.*[21] Interestingly the $N_{N=P}$–Cu bond lengths are rather different with the N–Cu1 bonds (N1–Cu1: 1.881(2) Å, N4–Cu1: 1.864(2) Å) being shorter than the N–Cu2 (N2–Cu2: 2.136(2) Å, N5–Cu2: 2.131(2) Å). Moreover a small d^{10}–d^{10} interaction between the two copper atoms may exist (Cu1–Cu2: 2.8863(3) Å),[22] based on DFT calculations (see ESI†).

In order to determine whether **3** remains dimeric in solution, ^{1}H DOSY experiments were performed on **2** and **3**. Their hydrodynamic radii were evaluated at 6.6 Å and 7.6 Å respectively. Approximating these complexes as a sphere gave volume

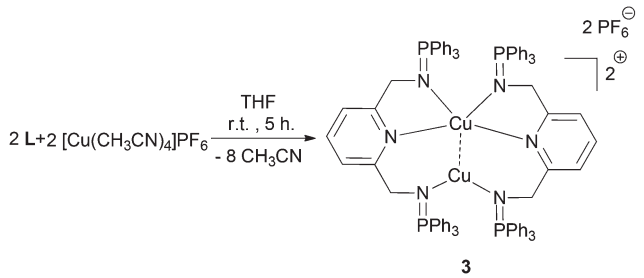

3

Scheme 3 Synthesis of $[L_2Cu_2]$.

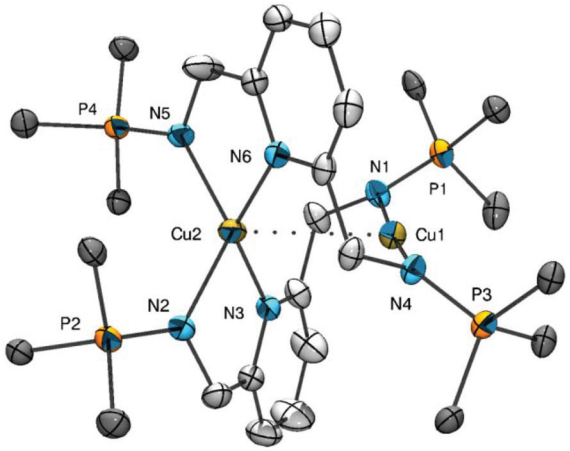

Fig. 5 ORTEP plot (50% of probability) of **3**, hydrogens and two PF_6^- counter-anions have been omitted for clarity, and phenyl substituents on P have been restricted to their C_{ipso} for the same reason. Selected bond lengths [Å] and angles (°): Cu1–Cu2 2.8863(3), N1–Cu1 1.881(2), N4–Cu1 1.867(2), N2–Cu2 2.136(2), N5–Cu2 2.131(2), N3–Cu2 2.012(2), N6–Cu2 2.011(2), P1–N1 1.587(2), P2–N2 1.582(2), N4–P3 1.597(2), N5–P4 1.594(2); N1–Cu1–N4 174.09(7), N5–Cu2–N6 83.41(6), N2–Cu2–N3 82.58(6), N2–Cu2–N5 129.23(6).

values comparable to those obtained by X-ray crystallography. This seems to indicate that the dimeric structure of **3** is maintained in solution; nevertheless, DFT calculations were conducted in order to evaluate the stability of this structure in the presence of the coordinating ligand. Enthalpy and Gibbs energy of the coordination reaction are reported in Fig. 6. As all the structures involved are cationic and the solvents used are polar (THF, acetonitrile), solvation effects were modelled with the polarisable continuum model (PCM).

These calculations show that the existence of the T-shaped complex (**VIII**) is unlikely, since the coordination of an acetonitrile ligand giving **VII** is favoured. Importantly, formation of the tetracoordinated (or tricoordinated, not depicted) cationic monomer with acetonitrile (**VII**) or an electron rich benzonitrile such as 1,3,5-trimethoxy-benzonitrile[23] (**VI**) is disfavoured compared to the dimer **V** by 18 and 10 kcal mol^{-1} respectively. This is in agreement with the results obtained from the ^{1}H DOSY NMR experiment. Experimentally, when mixing **3** and 1,3,5-trimethoxy-benzonitrile in acetonitrile no significant change was observed in $^{31}P\{^1H\}$ NMR. Moreover, X-ray analysis of single crystals obtained by gas diffusion of pentane evidenced the presence of **3**.

From these thermodynamic calculations, triethylphosphine should be able to react with **V** to give **IX** located 4 kcal mol^{-1} below the dimer **V**. Indeed when a suspension of **3** in THF is treated with an excess of PEt_3, the mixture turned rapidly clear to yield complex **4**, which was characterised by multinuclear NMR spectroscopy and X-ray analysis. Therefore, the formation of a monomeric complex requires a strong ancillary ligand (Br, PEt_3) (Scheme 4).

It is noteworthy that we used an excess of PEt_3 for practical reasons but never observed the decoordination of **L**. In the

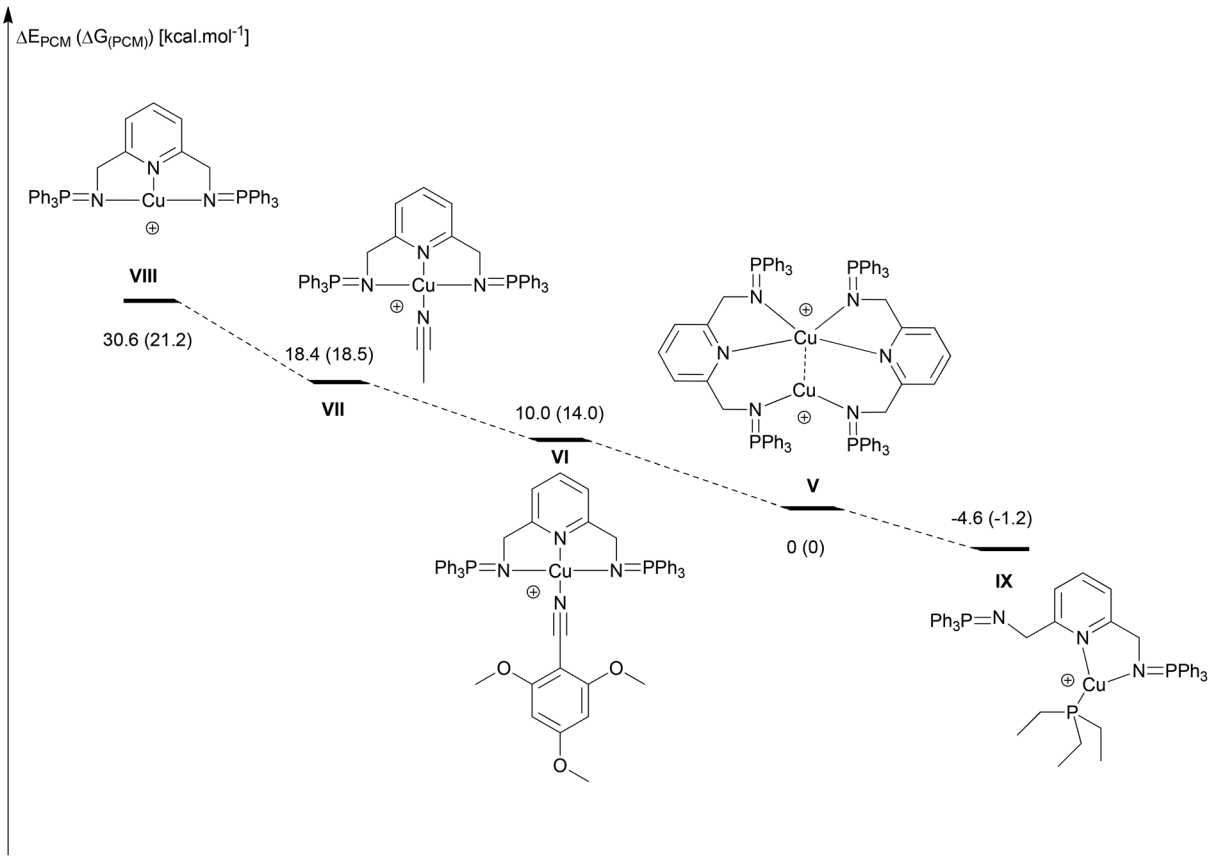

Fig. 6 Enthalpy and Gibbs energy of the coordination of various ligands on **V**.

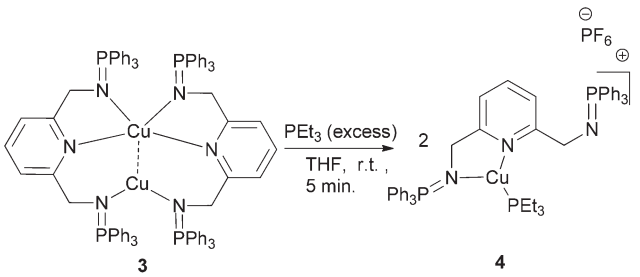

Scheme 4 Formation of **4** by addition of PEt_3.

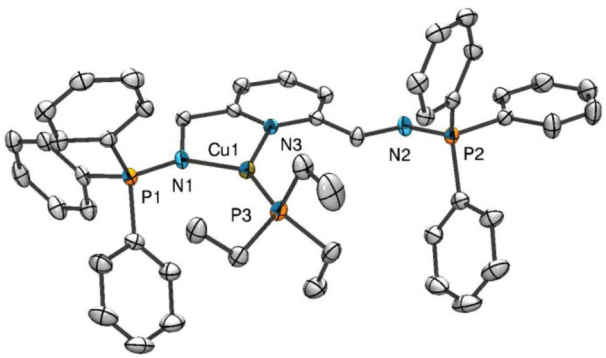

Fig. 7 ORTEP plot (50% of probability) of **4**, hydrogens and a PF_6^- counter-anion have been omitted for clarity. Selected bond lengths [Å] and angles (°): N1–Cu1 1.990(2), N3–Cu1 2.066(2), P1–N1 1.591(2), P2–N2 1.580(2), Cu1–P3 2.174(1); N1–Cu1–N3 83.1(1), N1–Cu1–P3 138.66(7).

$^{31}P\{^1H\}$ NMR spectrum both iminophosphorane moieties are equivalent appearing as a singlet at 21.6 ppm and the coordinated phosphine gave a singlet at −3.6 ppm. Therefore, room temperature ^1H, ^{13}C and ^{31}P NMR data seem to indicate a symmetric species in solution; however, no $^3J_{P,P}$ is observed on the $^{31}P\{^1H\}$ spectrum suggesting a dynamic behaviour as observed for **2**. VT-$^{31}P\{^1H\}$ NMR spectroscopy (see ESI†) allows the estimation of the activation barrier at 8.8(1) kcal mol^{-1}. Therefore, the hemilabile behaviour of **L** is maintained on a cationic copper(I) fragment. It is noteworthy that, X-ray analysis of single crystals formed by slow diffusion of pentane into its solution in THF gave a structure analogous to **2** (Fig. 7). The copper presents a trigonal geometry, the metal–nitrogen bond lengths and angles are comparable to those measured in **2**.

As the pincer coordination of bis(methyliminophosphoranyl)pyridine should be favoured on a copper(II) centre, we synthesised [LCu^{II}] complexes either by a chemical oxidation of **2** or a direct reaction of **L** with $CuBr_2$ (*vide infra*).

The cyclic voltammogram of **2** exhibits one irreversible oxidation wave at −0.36 V and one irreversible reduction wave at −0.93 V *vs.* $E^{1/2}(Fc^{+}/Fc)$ (see ESI†). We attributed the observed irreversibility to the rapid modification of the coordination mode of the ligand when changing the oxidation state of the copper atom. After oxidation, the second iminophosphorane coordinates with the metal and this pincer complex is then reduced inducing the rapid decoordination of one iminophosphorane group from the copper(I) centre. As anticipated the oxidation is slightly easier but the reduction is more difficult compared to that of (2-pyridylmethyl)imine copper(I) complexes.[24] In summary, both oxidation and reduction are irreversible but the sequence redox change/reorganisation can be repeated without loss of intensity.

Synthesis of copper(II) complexes

Prior to performing a chemical oxidation of **2**, we coordinated **L** to $CuBr_2$ (see Scheme 5). The reaction was conducted in THF, giving immediately a green solution. The green solid obtained after workup exhibits a singlet at 42.7 ppm in CD_2Cl_2 in $^{31}P\{^{1}H\}$ NMR but its ^{1}H NMR spectrum reveals broad and slightly shifted peaks suggesting a paramagnetic complex. This was further confirmed by the measurement of the magnetic moment of **5** by the Evans method[25] (μ_{eff} = 1.6(1)μ_B), in agreement with a S = 1/2 complex.

Crystals of **5** were obtained by slow evaporation of its THF solution, the structure is presented in Fig. 8. The copper is pentacoordinated and exhibits a nearly planar-square geometry (RMS deviation of 0.183 Å out of planarity) with a second bromine in the apical position, which is subjected to a Jahn–Teller distortion (Cu1–Br1 2.3599(6) Å *vs.* Cu1–Br2 2.9871(6) Å).

The two iminophosphorane bonds are similar (N1–P1 1.597(3), P2–N2 1.608(3)) and comparable to that observed in **2** for the coordinated iminophosphorane but significantly longer than the non-coordinated one in the same complex (1.565(3) in **2**).

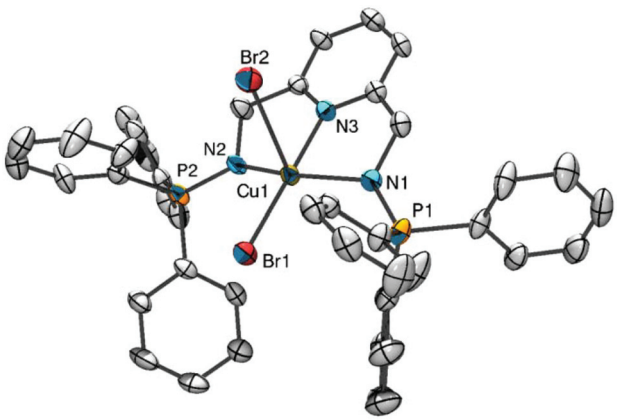

Fig. 8 ORTEP plot (50% of probability) of **5**, hydrogens have been omitted for clarity. Selected bond lengths [Å] and angles (°): N1–Cu1 2.041(3), N2–Cu1 2.071(3), N3–Cu1 1.955(3), P1–N1 1.597(3), P2–N2 1.608(3), Cu1–Br1 2.3599(6), Cu1–Br2 2.9871(6); N1–Cu1–N2 151.0(1), N3–Cu1–N1 79.6(1), N2–Cu1–N2 80.1(1), N3–Cu1–Br1 178.3(1), N3–Cu1–Br2 81.0(1).

Oxidation of copper(I) complex **2** was then realised with various oxidants ($NOBF_4$, $FcPF_6$, $[Ce(NO_3)_6](NH_4)_2$ (CAN), Scheme 5). In all cases, a rapid change to a green solution was observed, the product formed is characterised by a sharp singlet around 40 ppm by $^{31}P\{^{1}H\}$ NMR spectroscopy. From such a crude mixture obtained with CAN as the oxidant, single crystals were obtained. Their X-ray analysis evidenced a bimetallic $[\mathbf{L}Cu^{II}(CH_3CN)][Ce^{III}(NO_3)_5]$ complex **6** (see ESI†). The copper(II) complexes formed by oxidation were identified by the addition of KBr to give the independently synthesised complex **5** as ascertained by NMR spectroscopy and X-ray crystallography.

Thus, as expected no hemilability occurs on the more electron-deficient copper(II) centre, in agreement with a stronger interaction. Expecting that the versatile coordination of **L** may generate under-coordinated copper(I) species, complexes **2** and **3** were tested as catalysts in two well-known copper catalysed reactions (*i.e.* cyclopropanations and [3 + 2] cycloadditions).

Catalytic tests

As a test reaction we have examined the cyclopropanation[26] of styrene with EDA (ethyldiazoacetate) in the presence of 1% catalyst (Table 1). For comparable reactions, Reetz and coworkers have reported good conversion with a promising enantiomeric excess using a chiral iminophosphorane catalyst, suggesting that the donor iminophosphorane ligand remains bound to the metal during the catalysis.[27] This prompted us to evaluate complexes **2** and **3** in such reactions with the idea that they should be able to stabilise the copper carbene complex proposed as an intermediate in these cyclopropanation reactions.[28] First catalytic reactions with non-optimised conditions showed that complex **2** mainly catalyses the dimerisation of the diazo compound, while complex **3** is more efficient for cyclopropanation. However, in the presence of silver triflate, complex **2** becomes more selective. With a slower addition of EDA, we were able to obtain 85% of cyclopropane with **3** and above 90% with **2** after removal of the bromide.

Even if most cyclopropanation methodologies reported focused on the stereoselectivity of this process it is interesting to note that lower chemical yield of cyclopropane was obtained with copper complexes featuring diamine ligands.[29] In contrast to our expectation that the hemilability of the iminophosphorane arm could disfavour the dimerisation of the diazo compound, the addition of a poorly coordinating anion remains essential to control this side reaction. Therefore we decided not to further explore this process and turned our attention to [3 + 2] cycloadditions, another emblematic catalytic reaction with copper(I) catalysts.[30]

We first examined the cycloaddition of phenylacetylene and 4-methoxybenzylazide (Table 2). With 1% of both catalysts and without solvent, the reaction was very rapid and exothermic inducing a brutal solidification of the medium (Table 1, entry 1). Decreasing the amount of catalyst to 0.1% still allows a rapid reaction with a slower solidification of the medium. Full conversion is observed in this case within few minutes, the triazole was isolated in excellent yield (entries 2 and 3).

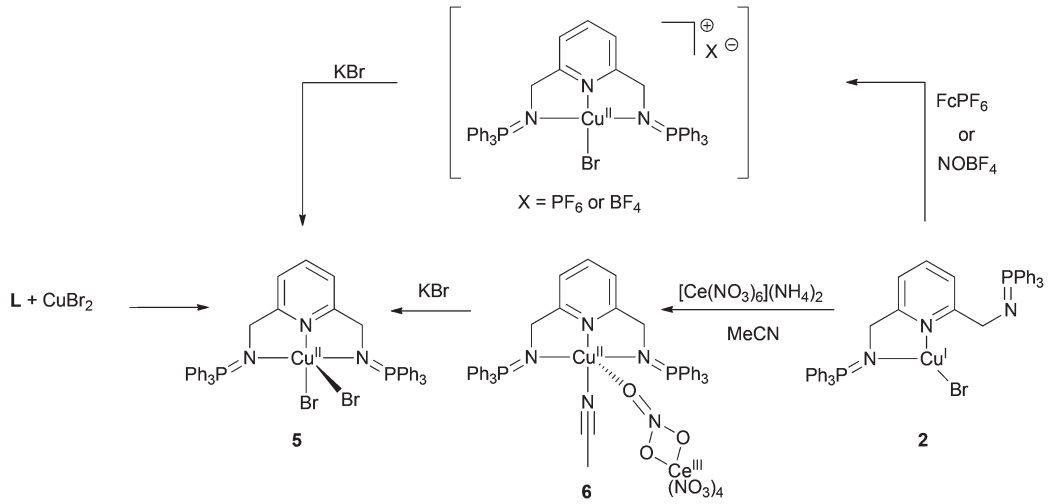

Scheme 5 Synthesis of copper(II) complexes by salt metathesis or chemical oxidation.

Table 1 Cyclopropanation reactions

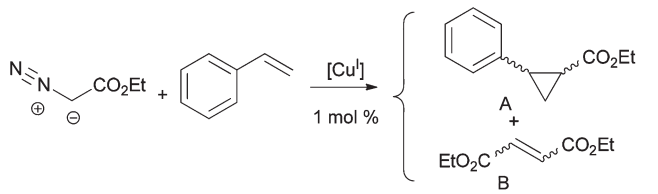

Catalyst	Additive[a]	Yield of A[b] (%)	Yield of B[b] (%)
3	None	85	15
2	AgOTf	93 (84)	7
2	$AgNTf_2$	91	9

[a] 1 mol%. [b] GC yield (isolated yield) with respect to EDA.

Table 2 [3 + 2] cycloaddition

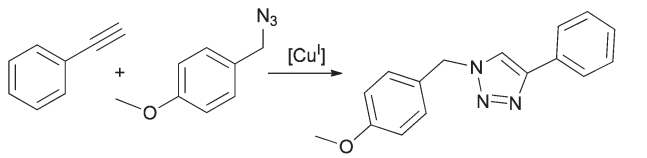

Catalyst	Conditions	Time	Yield[a]
2 or **3**	1 mol%, N_2, neat	<1 min	n.d.[b]
2	0.1 mol%, N_2, neat	3 min	94%
3	0.1 mol%, N_2, neat	5 min	98%
2	0.1 mol%, N_2, dichloromethane	20 min	96%
3	0.1 mol%, N_2, dichloromethane	30 min	98%
2	0.1 mol%, N_2, toluene	45 min	96%
3	0.1 mol%, N_2, toluene	2 h	95%
2	0.1 mol%, air, toluene/water	4 h	77%

[a] Isolated yield. [b] Not determined due to the very rapid solidification of the mixture.

Both catalysts allow also a rapid reaction in dichloromethane (entries 4 and 5). In toluene, **2** proved more efficient than **3** which is probably explained by its better solubility (entries 5 and 6). As both catalysts display comparable activity, further experiments were conducted with **2**. When carrying out this reaction in a biphasic toluene–water solvent mixture in air, we were pleased to observe that the catalyst remains active. The yield is lower compared to the anhydrous conditions, probably due to partial decomposition. Moreover, when reacting sterically hindered *tert*-butylacetylene with 4-methoxybenzylazide in the presence of 0.5% of **2**, the triazole was isolated in 98% yield after 2 h. These results are comparable to those described with bulky NHC–Cu(I) complexes;[31] however, 3-hexyne does not react in the presence of **2**. Therefore the cycloaddition proceeds efficiently at a low catalyst loading even with a less reactive alkyne, these performances outstrip those of $[CuBr(PPh_3)_3]$[32] or of other iminophosphorane systems.[33]

Conclusion

In conclusion, we evidenced the versatile coordination of bis-(methyliminophosphoranyl)pyridine ligand **L** to copper centres depending on both the oxidation state of the Cu and the reaction conditions. Generally only one iminophosphorane is bound to the metal in copper(I) complexes, and these monomeric complexes (**2** and **4**) exhibit a fluxional behaviour in solution, which was studied by variable temperature NMR and/or DFT calculations. When no strong coordinating ligand is available a dimeric complex **3** is formed whose structure is preserved in solution. The oxidation of [**L**CuBr] is irreversible and induces a change in the coordination mode of **L**. Indeed in copper(II) complex **5**, which has been synthesised by chemical oxidation of **2** or from $CuBr_2$, **L** acts as a pincer. Therefore the hemilability of the iminophosphorane moieties can be redox driven. In order to evaluate their catalytic ability copper(I) complexes **2** and **3** were employed for cyclopropanation and [3 + 2] cycloaddition of organic azides on alkynes. Current efforts focus on exploring this switchable redox-induced hemilability with other late transition metals.

Experimental part

Synthesis

All reactions were conducted under an atmosphere of dry nitrogen or argon, using standard Schlenk and glovebox techniques. Solvents and reagents were obtained from commercial sources. Tetrahydrofuran, diethyl ether, toluene and petroleum ether were dried with an MBraun MB-SPS 800 solvent purification system. Pentane and acetonitrile were distilled from CaH_2, under dry nitrogen. $[CuBr(PPh_3)_3]$[34] and $[CuBr(SEt_2)]$[35] were prepared following the literature procedure.

Measurements

Nuclear magnetic resonance (NMR) spectra were recorded on a Bruker Av300 spectrometer operating at 300 MHz for ^1H, 75.5 MHz for ^{13}C, and 121.5 MHz for ^{31}P. Solvent peaks were used as internal references for ^1H and ^{13}C chemical shifts (ppm). ^{31}P peaks were referenced to an external 85% H_3PO_4. The following abbreviations are used: br, broad; s, singlet; d, doublet; t, triplet; m, multiplet; hept, heptuplet. Labelling of atoms is indicated in Scheme 1. It should be mentioned that solution ^{31}P chemical shift of the compounds described herein can be remarkably affected by the nature of the solvent and, to a lesser extent, by dilution.[36]

The ^1H PGSE (DOSY) experiments were performed on the same spectrometer. The experiment was measured using the ledbpgp2s pulse program (Bruker) at a temperature of 298 K. A relaxation delay of 10 s was employed along with a diffusion time (Δ) of 50 ms and an eddy current delay of 5 ms. Bipolar gradient pulses ($\delta/2$) of 2.2 ms and homospoil gradient pulses of 1.1 ms were used. The gradient strengths of the 2 homospoil pulses were −17.13% and −13.17%, respectively. Thirty-two experiments of sixteen scans each were collected with the bipolar gradient strength, initially at 2% (1st experiment), linearly increased to 95% (32nd experiment). All gradient pulses were sine shaped and after each application a recovery delay of 200 μs was used. Further processing was achieved using the MestReNova software.

MAS (magic angle spinning) ^{31}P solid-state NMR experiments were recorded at room temperature on a Tecmag Apollo360 spectrometer using a CP/MAS Bruker probe. The ^{31}P spectrum (Larmor frequency: 145.77 MHz, spinning rotation: 15 kHz) was externally referenced to a solution of H_3PO_4.

Elemental analyses were determined by Mr Stephen Boyer at London Metropolitan University.

Synthesis of dibromomethylpyridine. Adapted from a literature procedure:[37] 2,6-dihydroxymethylpyridine (3.48 g, 25 mmol) was dissolved in 50 mL of DMF. The flask was cooled to 0 °C and PBr_3 (57.5 mmol, 5.5 mL) was added dropwise under vigorous stirring. The ice bath was removed and the mixture was stirred overnight. Water (125 mL) was slowly added to quench the reaction, the mixture was extracted with Et_2O (3 × 125 mL), the combined organic layers were washed with water (2 × 150 mL) and brine (150 mL), dried over $MgSO_4$ and evaporated to dryness giving an off-white solid (6.03 g, 91%). ^1H NMR ($CDCl_3$) δ 7.70 (t, J = 8.0 Hz, 1H, H_1), 7.37 (d, J = 8.0 Hz, 2H, H_2), 4.53 (s, 4H, H_4). ^{13}C NMR ($CDCl_3$) δ 156.8 (C_3), 138.3 (C_1), 122.4 (C_2), 33.6 (C_4).

Synthesis of 1. NaN_3 (0.813 g, 12.5 mmol) was dissolved in DMSO (25 mL), dibromomethylpyridine (1.33 g, 5 mmol) was added and the mixture was stirred overnight at room temperature. Water (25 mL) was added to quench the reaction, the mixture was then extracted with Et_2O (3 × 50 mL), the combined organic layers were washed with water (2 × 100 mL) and brine (100 mL), dried over $MgSO_4$ and evaporated to dryness to yield **1** as a yellow oil (0.940 g, 99%). ^1H NMR ($CDCl_3$) δ 7.76 (t, J = 8.0 Hz, 1H, H_1), 7.30 (d, J = 8.0 Hz, 2H, H_2), 4.48 (s, 4H, H_4). ^{13}C NMR ($CDCl_3$) δ 155.9 (C_3), 138.0 (C_1), 121.1 (C_2), 55.4 (C_4).

Synthesis of L. In a Schlenk flask, **1** (1.40 g, 7.40 mmol) and PPh_3 (3.88 g, 14.8 mmol) were mixed in dry Et_2O (70 mL) inducing nitrogen evolution. The mixture was stirred overnight at room temperature (if necessary the flask can be evacuated after few minutes to avoid over-pressure). The completeness of the reaction was verified by $^{31}P\{^1H\}$ NMR showing a singlet at 6.6 ppm for the bis(iminophosphorane). The reaction volume was reduced to about 15 mL resulting in the formation of a white precipitate which was filtered under nitrogen, washed with pentane (2 × 30 mL) and dried under vacuum to yield **3** (4.23 g, 87%). $^{31}P\{^1H\}$ NMR (CD_2Cl_2) δ 9.9 (s). ^1H (CD_2Cl_2) δ 7.79–7.59 (m, 15H, H_1, H_2, and H_6), 7.57–7.30 (m, 18H, H_7, H_8), 4.30 (d, $J_{P,H}$ = 16.0 Hz, 4H, H_4). ^{13}C NMR (CD_2Cl_2) δ 164.4 (d, $J_{C,H}$ = 23.5 Hz, C_3), 136.7 (C_1), 132.8 (d, $J_{P,C}$ = 9.0 Hz, C_6), 132.4 (d, $J_{P,C}$ = 95.5 Hz, C_5), 131.5 (d, $J_{P,C}$ = 3.0 Hz, C_8), 128.7 (d, C, $J_{P,C}$ = 11.5 Hz, C_7), 118.5 (C_2), 51.4 (d, $J_{P,C}$ = 3.0 Hz, C_4). Anal. Calcd for $C_{43}H_{37}N_3P_2$: C, 78.52; H, 5.67; N, 6.39. Found: 78.39; H, 5.74; N, 6.49.

Synthesis of [LCuBr] (2). From CuBr: **L** (0.917 g, 1.39 mmol) and CuBr (0.200 g, 1.39 mmol) were mixed in THF (10 mL) and heated overnight at 50 °C, the mixture turned yellow with the formation of a clear yellow precipitate. The completeness of the reaction was ascertained by $^{31}P\{^1H\}$ NMR, then the solvent volume was reduced to about 5 mL, and 10 mL of pentane were added to achieve the precipitation. The resulting mixture was centrifuged, the supernatant was removed, the solid was washed twice with pentane (10 mL) and finally dried under vacuum overnight to yield the title compound as a clear yellow powder (1.05 g, 94%). $^{31}P\{^1H\}$ NMR (THF-d^8) δ 16.5 (bs). ^1H NMR (CD_3CN) δ 7.77 (t, $J_{H,H}$ = 7.7 Hz, 1H, H_1), 7.64–7.08 (m, 30H, H_6, H_7, H_8), 7.04 (d, $J_{H,H}$ = 7.7 Hz, 2H, H_2), 4.13 (d, $J_{P,H}$ = 11.1 Hz, 4H, H_4). ^{13}C NMR (CD_3CN) δ 161.6 (d, $J_{P,C}$ = 19.0 Hz, C_3), 138.6 (C_1), 133.7 (C_8), 133.6 ($J_{P,C}$ = 9.5 Hz, C_6), 129.8 ($J_{P,C}$ = 12.0 Hz, C_7), 128.3 ($J_{P,C}$ = 98.8 Hz, C_5), 122.6 (C_2), 53.2 (C_4). Anal. Calcd for $C_{43}H_{37}BrCuN_3P_2$: C, 64.46; H, 4.65; N, 5.24. Found: C, 64.31; H, 4.66; N, 5.17.

From $[CuBr(SEt_2)]$: 23.4 mg of $[CuBr(SEt_2)]$ (23.4 mg, 0.1 mmol) and of **L** (65.8 mg, 0.1 mmol) were stirred in THF (5 mL) for 2 hours. **2** was obtained after precipitation and repeated washing with pentane (5 × 3 mL) (43.3 mg, 54%).

From $[CuBr(PPh_3)_3]$: **L** (0.131 g, 0.2 mmol) and $[CuBr(PPh_3)_3]$ (0.186 g, 0.2 mmol) were stirred in THF (5 mL) for 2 hours, the completeness of the reaction was verified by

$^{31}P\{^{1}H\}$ NMR showing **2**, and the presence of free PPh_3 (δ_p = −5.2 ppm). The solvent was evaporated and the resulting solid was washed with Et_2O (6 × 5 mL), finally **2** was obtained as a slightly yellow powder (64.2 mg, 40%).

Complex $[L_2Cu_2](PF_6)_2$ (3). In a Schlenk flask, **L** (131.5 mg, 0.2 mmol) and $[Cu(CH_3CN)_4]PF_6$ (74.4 mg, 0.2 mmol) were dissolved in THF (5 mL), the solution turned quickly to yellow/green and was stirred for one additional hour upon which a yellow precipitate formed. The completeness of the reaction was checked by $^{31}P\{^{1}H\}$ NMR of the crude mixture. The solvent was reduced to about 1 mL and 10 mL of petroleum ether were added to complete the precipitation, the solid was separated by filtration, washed with Et_2O (5 mL) and petroleum ether (10 mL). The resulting yellow solid was dried under vacuum overnight to give **3** (147 mg, 85%). $^{31}P\{^{1}H\}$ NMR (CD_3CN) δ 30.8 (s), −142.2 (hept, J_{PF} = 706 Hz). ^{1}H NMR (CD_3CN) δ 7.78 (t, $J_{H,H}$ = 7.5 Hz, 1H, H_1), 7.55–7.41 (m, 6H, H_8), 7.38–7.25 (m, 12H, H_6), 7.20–7.16 (m, 12H, H_7), 6.98 (d, $J_{H,H}$ = 7.8 Hz, 2H, H_2), 4.12 (bs, 4H, H_4). ^{13}C NMR ($CDCl_3$) δ 161.7 (d, $J_{C,P}$ = 17.6 Hz, C_3), 138.9 (C_1), 134.0 ($J_{C,P}$ = 2.9 Hz, C_8), 133.8 ($J_{C,P}$ = 9.5 Hz, C_6), 130.0 (d, $J_{C,P}$ = 12.1 Hz, C_7), 128.1 ($J_{C,P}$ = 99.1 Hz, C_5), 123.2 (C_2), 53.7 (C_4). Anal. Calcd for $C_{86}H_{74}Cu_2F_{12}N_6P_6$: C, 59.62; H, 4.31; N, 4.85. Found: C, 59.51; H, 4.41; N, 4.82.

From **2**: Using a vial, **2** (9.1 mg, 11.4 μmol) and $AgPF_6$ (2.9 mg, 11.4 μmol) were mixed in THF-d_8 (1 mL) inducing the rapid precipitation of the formed AgBr salt. The mixture is filtered and transferred to an NMR tube for spectroscopic analysis which was in agreement with the data reported above. The yield was not determined.

Complex $[LCu(PEt_3)]PF_6$ (4). In a vial, PEt_3 (25 mg, 0.21 mmol) was added to $[L_2Cu_2](PF_6)_2$ (64.9 mg 0.038 mmol) suspended in THF (2 mL), within few seconds the solution turned clear. The solution was layered with pentane and allowed to stand overnight at −35 °C to yield colorless crystals which were collected, washed with pentane (5 mL) and dried in a vacuum (29 mg, 39%). $^{31}P\{^{1}H\}$ NMR (THF-d^8) δ 21.6 (s, P^V), −3.4 (s, P^{III}), −144.8 (hept, J_{PF} = 710 Hz, PF_6). ^{1}H NMR (THF-d^8) δ 7.89–7.73 (m, 13H, H_1, H_6), 7.72–7.48 (m, 20H, H_2, H_7, H_8), 4.46 (d, $J_{P,H}$ = 10.0 Hz, 4H, H_4), 0.92 (t, $J_{H,H}$ = 7.5 Hz, 6H, PCH_2CH_3), 0.69 (dt, $J_{P,H}$ = 15.5 Hz, $J_{H,H}$ = 7.5 Hz, 9H, PCH_2CH_3). ^{13}C NMR (THF-d^8) δ 163.5 (d, $J_{C,P}$ = 24.0 Hz, C_3), 139.0 (C_1), 133.5 (d, $J_{C,P}$ = 9.0 Hz, C_6), 133.1 (d, $J_{C,P}$ = 3.0 Hz, C_8), 130.5 (d, $J_{C,P}$ = 98.0 Hz, C_5), 129.6 (d, $J_{C,P}$ = 11.5 Hz, C_7), 120.7 (C_2), 53.3 (C_4), 16.3 (d, $J_{C,P}$ = 23.7 Hz, CH_2), 8.7 (d, $J_{C,P}$ = 1.4 Hz, CH_3). Anal. Calcd for $C_{49}H_{52}CuF_6N_3P_4$: C, 59.79; H, 5.32; N, 4.27. Found: C, 59.65; H, 5.32; N, 4.36.

Complex $[LCuBr_2]$ (5). **L** (131.5 mg, 0.2 mmol) was suspended in THF (10 mL) and anhydrous $CuBr_2$ (44.7 mg, 0.2 mmol) was added. The mixture turned immediately green and after 30 minutes of stirring a green precipitate formed. The solvent is evaporated under vacuum, the solid is washed with Et_2O (2 × 5 mL), dried under vacuum overnight to give the title compound as a green powder (104.5 mg, 59%). $^{31}P\{^{1}H\}$ (CD_2Cl_2) δ 42.7 (s). μ_{eff} = 1.6μ_B (by the Evans method in CD_2Cl_2). Anal. Calcd for $C_{43}H_{37}Br_2CuN_3P_2$: C, 58.62; H, 4.23; N, 4.77. Found: C, 58.30; H, 4.38; N, 4.62.

General catalytic protocols for [3 + 2] cycloaddition

In a glove-box, a Schlenk flask was charged with the catalyst (1 mol% or 0.1 mol%), the flask was closed and removed from the glove-box. Under a flux of nitrogen, the solvent or the mixture of solvents (1 mL) was added, and then the azide (1 mmol, 154 μL) and the alkyne (1 mmol, 110 μL) were introduced. Depending on the reaction conditions, the flask was either closed, evacuated and back-filled with nitrogen or let to open air. The completion of the reaction was checked by TLC. The reaction was quenched by the addition of water (5 mL), extracted with EtOAc (3 × 5 mL), dried over $MgSO_4$ and subjected to rotary evaporation to yield the triazole.

1-(4′-Methoxybenzyl)-4-phenyl-1*H*-1,2,3-triazole (94%). Spectroscopic data were in agreement with the literature.[38] The compound was also univocally identified by X-ray analysis of crystals obtained by slow evaporation of the NMR sample (X-ray structure is available on request).

1-(4′-Methoxybenzyl)-4-*t*butyl-1*H*-1,2,3-triazole (98%). ^{1}H NMR ($CDCl_3$) δ 7.22 (d, J = 8.5 Hz, 2H, H_{Ar}), 7.11 (s, 1H, $H_{triazole}$), 6.89 (d, J = 8.5 Hz, 2H, H_{Ar}), 5.41 (s, 2H, CH_2), 3.81 (s, 3H, OMe), 1.31 (s, 9H, *t*Bu). ^{13}C NMR ($CDCl_3$) δ 159.96 (C^{IV}_{Ar}), 158.21 (C^{IV}_{Ar}), 129.74 (CH_{Ar}), 127.19 ($C^{IV}_{triazole}$), 118.21 ($CH_{triazole}$), 114.55 (CH_{Ar}), 55.46 (OMe), 53.63 (CH_2), 30.9 (C^{IV}-*t*Bu) 30.51 (*t*Bu).

General optimised catalytic protocols for cyclopropanation

In a glove-box, a Schlenk flask was charged with the catalyst (1 mol%) and the silver salt (1 mol%). The flask was closed and removed from the glove-box. Under a flux of nitrogen, dry CH_2Cl_2 (3 mL) and styrene (460 μL, 4 mmol) were added using a syringe, then the flask was cooled to about −5 °C and the EDA (2 mmol, 210 μL) diluted in 5 mL of dry CH_2Cl_2 was added dropwise over 1 h. The flask was then closed, evacuated and back-filled with nitrogen and stirred overnight. The mixture was analyzed by GC. The solvent was then evaporated to yield the crude mixture which was purified by flash chromatography (95/5 petroleum ether–EtOAc) to give a mixture of diastereoisomers with NMR data in agreement with the literature.[39]

X-ray crystallography

Data were collected at 150 K on a Bruker Kappa APEX II diffractometer using a Mo-Kα (λ = 0.71069 Å) X-ray source and a graphite monochromator. The crystal structure was solved using SIR 97[40] and SHELXL-97 or SHELXL-2013.[41] ORTEP drawings were made using ORTEP III for Windows.[42] X-ray data are gathered in Table S1 (ESI†).

Computational details

All calculations were performed using the Gaussian 09 series of programs (revision B.01).[43] The ω-B97XD functional was used in combination with the 6-31G* basis set for carbons and hydrogens; the 6-311+G** basis set for bromine, phosphorus, nitrogen and oxygen; and the Def2-TZVP basis set for copper.[44] The stationary points and transition states were characterised

by full vibration frequency calculations, with no imaginary frequency for minima (stationary point), and one imaginary frequency for the transition states. Solvent effects were introduced through PCM single-point calculations,[45] using standard Gaussian parameters, the solvent was THF. The PCM Gibbs energies were calculated using the correction proposed by Maseras and coworkers.[46]

Acknowledgements

Ecole Polytechnique and CNRS are thanked for financial support. We are grateful to Dr S. Maron for recording MAS ^{31}P NMR, Dr E. Nicolas and Dr S. Labouille for fruitful discussions about DFT calculations and Dr G. Nocton for his help on VT and DOSY NMR.

Notes and references

1 M. Albrecht and G. van Koten, *Angew. Chem., Int. Ed.*, 2001, **40**, 3750–3781.
2 *The chemistry of pincer ligands*, ed. D. Morales-Morales and C. Jensen, Elsevier, 2007.
3 D. Benito-Garagorri, M. Puchberger, K. Mereiter and K. Kirchner, *Angew. Chem., Int. Ed.*, 2008, **47**, 9142–9145; P. O'Leary, C. A. van Walree, N. C. Mehendale, J. Sumerel, D. E. Morse, W. C. Kaska, G. van Koten and R. Gebbink, *Dalton Trans.*, 2009, 4289–4291; B. Wieczorek, H. P. Dijkstra, M. R. Egmond, R. Gebbink and G. van Koten, *J. Organomet. Chem.*, 2009, **694**, 812–822.
4 S. Wanniarachchi, B. J. Liddle, J. Toussaint, S. V. Lindeman, B. Bennett and J. R. Gardinier, *Dalton Trans.*, 2010, **39**, 3167–3169; C. H. Wang, N. N. Ma, X. X. Sun, S. L. Sun, Y. Q. Qiu and P. J. Liu, *J. Phys. Chem. A*, 2012, **116**, 10496–10506; Q. Q. Wang, R. A. Begum, V. W. Day and K. Bowman-James, *Inorg. Chem.*, 2012, **51**, 760–762.
5 D. Benito-Garagorri and K. Kirchner, *Acc. Chem. Res.*, 2008, **41**, 201–213; J. M. Serrano-Becerra and D. Morales-Morales, *Curr. Org. Synth.*, 2009, **6**, 169–192; N. Selander and K. J. Szabo, *Chem. Rev.*, 2011, **111**, 2048–2076; C. Gunanathan and D. Milstein, *Acc. Chem. Res.*, 2011, **44**, 588–602; D. Gelman and S. Musa, *ACS Catal.*, 2012, **2**, 2456–2466; G. van Koten, *J. Organomet. Chem.*, 2013, **730**, 156–164.
6 R. Lindner, B. v. d. Bosch, M. Lutz, J. N. H. Reek and J. I. van der Vlugt, *Organometallics*, 2011, **30**, 499–510.
7 L. Flamigni, J. P. Collin and J. P. Sauvage, *Acc. Chem. Res.*, 2008, **41**, 857–871; R. Sakamoto, S. Katagiri, H. Maeda and H. Nishihara, *Coord. Chem. Rev.*, 2013, **257**, 1493–1506.
8 V. C. Gibson, C. Redshaw and G. A. Solan, *Chem. Rev.*, 2007, **107**, 1745–1776; P. J. Chirik and K. Wieghardt, *Science*, 2010, **327**, 794–795; C. Carmen, H. Atienza, C. Milsmann, S. P. Semproni, Z. R. Turner and P. J. Chirik, *Inorg. Chem.*, 2013, **52**, 5403–5417.
9 S. Al-Benna, M. J. Sarsfield, M. Thornton-Pett, D. L. Ormsby, P. J. Maddox, P. Brès and M. Bochmann, *J. Chem. Soc., Dalton Trans.*, 2000, 4247–4257.
10 Z. Y. Chai, C. Zhang and Z. X. Wang, *Organometallics*, 2008, **27**, 1626–1633; Z. Y. Chai and Z. X. Wang, *Dalton Trans.*, 2009, 8005–8012.
11 M. J. Sgro and S. W. Stephan, *Dalton Trans.*, 2011, **40**, 2419–2421.
12 Transition metal P-N complexes as polymerization catalysts by LANXESS Deutschland GmbH and University of Toronto, EP2641909, 2013.
13 L. P. Spencer, R. Altwer, P. R. Wei, L. Gelmini, J. Gauld and D. W. Stephan, *Organometallics*, 2003, **22**, 3841–3854.
14 R. Bielsa, R. Navarro, E. P. Urriolabeitia and T. Soler, *Dalton Trans.*, 2008, 1203–1214; D. Aguilar, M. Contel, R. Navarro, T. Soler and E. P. Urriolabeitia, *J. Organomet. Chem.*, 2009, **694**, 486–493; N. Lease, V. Vasilevski, M. Carreira, A. de Almeida, M. Sanau, P. Hirva, A. Casini and M. Contel, *J. Med. Chem.*, 2013, **56**, 5806–5818.
15 P. Braunstein and F. Naud, *Angew. Chem., Int. Ed.*, 2001, **40**, 680–699.
16 J. Garcia-Alvarez, S. E. Garcia-Garrido and V. Cadierno, *J. Organomet. Chem.*, 2014, **751**, 792–808.
17 T. Miekisch, H. J. Mai, R. Meyer, R. M. Z. Kocker, K. Dehnicke, J. Magull and H. Goesmann, *Z. Anorg. Allg. Chem.*, 1996, **622**, 583–588; S. Wingerter, H. Gornitzka, G. Bertrand and D. Stalke, *Eur. J. Inorg. Chem.*, 1999, 173–178; T. K. Panda, P. W. Roesky, P. Larsen, S. Zhang and C. Wickleder, *Inorg. Chem.*, 2006, **45**, 7503–7508; G. B. Ma, M. J. Ferguson, R. McDonald and R. G. Cavell, *Organometallics*, 2010, **29**, 4251–4264.
18 M. J. Sarsfield, I. May, S. M. Cornet and M. Helliwell, *Inorg. Chem.*, 2005, **44**, 7310–7312; B. Liu, D. Cui, J. Ma, X. Chen and X. Jing, *Chem. – Eur. J.*, 2007, **13**, 834–845; K. R. D. Johnson and P. G. Hayes, *Organometallics*, 2009, **28**, 6352–6361; D. Li, S. Li, D. Cui, X. Zhang and A. A. Trifonov, *Dalton Trans.*, 2011, **40**, 2151–2153; Z. Jian, W. Rong, Z. Mou, Y. Pan, H. Xie and D. Cui, *Chem. Commun.*, 2012, **48**, 7516–7518; H. Sun, J. S. Ritch and P. G. Hayes, *Dalton Trans.*, 2012, **41**, 3701–3713.
19 M. Demange, L. Boubekeur, A. Auffrant, N. Mezailles, L. Ricard, X. Le Goff and P. Le Floch, *New J. Chem.*, 2006, **30**, 1745–1754; A. Buchard, H. Heuclin, A. Auffrant, X. F. Le Goff and P. Le Floch, *Dalton Trans.*, 2009, 1659–1667; T. P. A. Cao, S. Labouille, A. Auffrant, Y. Jean, X. F. Le Goff and P. Le Floch, *Dalton Trans.*, 2011, **40**, 10029–10037.
20 J. I. van der Vlugt, E. A. Pidko, D. Vogt, M. Lutz, A. L. Spek and A. Meetsma, *Inorg. Chem.*, 2008, **47**, 4442–4444; J. I. van der Vlugt, E. A. Pidko, D. Vogt, M. Lutz and A. L. Spek, *Inorg. Chem.*, 2009, **48**, 7513–7515.
21 C. Piguet, G. Bernardinelli and A. F. Williams, *Inorg. Chem.*, 1989, **28**, 2920–2925.
22 S. Sculfort and P. Braunstein, *Chem. Soc. Rev.*, 2011, **40**, 2741–2760.

23 M. Raducan, C. Rodriguez-Escrich, X. C. Cambeiro, E. C. Escudero-Adan, M. A. Pericas and A. M. Echavarren, *Chem. Commun.*, 2011, **47**, 4893–4895.
24 S. A. Turner, Z. D. Remillard, D. T. Gijima, E. Gao, R. D. Pike and C. Goh, *Inorg. Chem.*, 2012, **51**, 10762–10773.
25 D. F. Evans, *J. Chem. Soc.*, 1959, 2003–2005; J. L. Deutsch and S. M. Poling, *J. Chem. Educ.*, 1969, **46**, 167; J. Loliger and R. Scheffol, *J. Chem. Educ.*, 1972, **49**, 646–647; D. H. Grant, *J. Chem. Educ.*, 1995, **72**, 39–40.
26 H. Lebel, J. F. Marcoux, C. Molinaro and A. B. Charette, *Chem. Rev.*, 2003, **103**, 977–1050; M. Yu and B. L. Pagenkopf, *Tetrahedron*, 2005, **61**, 321–347; B. Morandi and E. M. Carreira, *Science*, 2012, **335**, 1471–1474.
27 M. T. Reetz, E. Bohres and R. Goddard, *Chem. Commun.*, 1998, 935–936.
28 I. V. Shishkov, F. Rominger and P. Hofmann, *Organometallics*, 2009, **28**, 1049–1059; P. Hofmann, I. V. Shishkov and F. Rominger, *Inorg. Chem.*, 2008, **47**, 11755–11762; W. Kirmse, *Angew. Chem., Int. Ed.*, 2003, **42**, 1088–1093.
29 D. J. Cho, S. J. Jeon, H. S. Kim, C. S. Cho, S. C. Shim and T. J. Kim, *Tetrahedron: Asymmetry*, 1999, **10**, 3833–3848; Y. Imai, W. B. Zhang, T. Kida, Y. Nakatsuji and I. Ikeda, *J. Org. Chem.*, 2000, **65**, 3326–3333.
30 V. V. Rostovtsev, L. G. Green, V. V. Fokin and K. B. Sharpless, *Angew. Chem., Int. Ed.*, 2002, **41**, 2596–2599; S. Diez-Gonzalez, *Catal. Sci. Technol.*, 2011, **1**, 166–178.
31 S. Diez-Gonzalez, A. Correa, L. Cavallo and S. P. Nolan, *Chem. – Eur. J.*, 2006, **12**, 7558–7564; S. Diez-Gonzalez, E. C. Escudero-Adan, J. Benet-Buchholz, E. D. Stevens, A. M. Z. Slawin and S. P. Nolan, *Dalton Trans.*, 2010, **39**, 7595–7606; S. C. Sau, S. R. Roy, T. K. Sen, D. Mullangi and S. K. Mandal, *Adv. Synth. Catal.*, 2013, **355**, 2982–2991.
32 S. Lal and S. Diez-Gonzalez, *J. Org. Chem.*, 2011, **76**, 2367–2373.
33 J. Garcia-Alvarez, J. Diez, J. Gimeno, F. J. Suarez and C. Vincent, *Eur. J. Inorg. Chem.*, 2012, 5854–5863.
34 R. Gujadhur, D. Venkataraman and J. T. Kintigh, *Tetrahedron Lett.*, 2001, **42**, 4791–4793.
35 M. Knorr, A. Pam, A. Khatyr, C. Strohmann, M. M. Kubicki, Y. Rousselin, S. M. Aly, D. Fortin and P. D. Harvey, *Inorg. Chem.*, 2010, **49**, 5834–5844.
36 M. Pomerantz, B. T. Ziemnicka, Z. M. Merchant, W. N. Chou, W. B. Perkins and S. Bittner, *J. Org. Chem.*, 1985, **50**, 1757–1759.
37 S. Abada, A. Lecointre, M. Elhabiri and L. J. Charbonniere, *Dalton Trans.*, 2010, **39**, 9055–9062.
38 Y. M. A. Yamada, S. M. Sarkar and Y. Uozumi, *J. Am. Chem. Soc.*, 2012, **134**, 9285–9290.
39 M. P. A. Lyle and P. D. Wilson, *Org. Lett.*, 2004, **6**, 855–857.
40 A. Altomare, M. C. Burla, M. Camalli, G. L. Cascarano, C. Giacovazzo, A. Guagliardi, A. G. G. Moliterni, G. Polidori and R. Spagna, *J. Appl. Crystallogr.*, 1999, **32**, 115–119.
41 G. M. Sheldrick, *SHELXL-97*, Universität Göttingen, Göttingen, Germany, 1997.
42 L. J. Farrugia, *ORTEP-3 program*, Department of Chemistry, University of Glasgow, 2001.
43 M. J. Frisch, *et al.*, *GAUSSIAN 09 (Revision B.01)*, Wallingford CT, 2010.
44 F. Weigend and R. Ahlrichs, *Phys. Chem. Chem. Phys.*, 2005, **7**, 3297–3305.
45 S. Miertus, E. Scrocco and J. Tomasi, *Chem. Phys.*, 1981, **55**, 117–129.
46 A. A. C. Braga, G. Ujaque and F. Maseras, *Organometallics*, 2006, **25**, 3647–3658.